

DIRECT EVIDENCE FOR HADRONIC COSMIC-RAY ACCELERATION IN THE SUPERNOVA REMNANT IC 443

M. TAVANI^{1,2}, A. GIULIANI³, A. W. CHEN^{3,4}, A. ARGAN¹, G. BARBIELLINI⁵, A. BULGARELLI⁶, P. CARAVEO³, P. W. CATTANEO⁷,
V. COCCO¹, T. CONTESSI³, F. D’AMMANDO^{1,2}, E. COSTA¹, G. DE PARIS¹, E. DEL MONTE¹, G. DI COCCO⁶, I. DONNARUMMA¹,
Y. EVANGELISTA¹, A. FERRARI^{4,8}, M. FEROCI¹, F. FUSCHINO⁶, M. GALLI⁹, F. GIANOTTI⁶, C. LABANTI⁶, I. LAPSHOV¹,
F. LAZZAROTTO¹, P. LIPARI¹⁰, F. LONGO⁵, M. MARISALDI⁶, M. MASTROPIETRO¹¹, S. MEREGHETTI³, E. MORELLI⁶, E. MORETTI⁵,
A. MORSELLI¹², L. PACCIANI¹, A. PELLIZZONI¹³, F. PEROTTI³, G. PIANO^{1,2,12}, P. PICOZZA^{2,12}, M. PILIA¹⁴, G. PUCELLA¹⁵,
M. PREST¹⁴, M. RAPISARDA¹⁵, A. RAPPOLDI⁷, E. SCALISE¹, A. RUBINI¹, S. SABATINI^{2,12}, E. STRIANI^{2,12}, P. SOFFITTA¹,
M. TRIFOGLIO⁶, A. TROIS¹, E. VALLAZZA⁵, S. VERCELLONE¹⁶, V. VITTORINI^{1,2}, A. ZAMBRA³, D. ZANELLO¹⁰, C. PITTORI¹⁷,
F. VERRECCHIA¹⁷, P. SANTOLAMAZZA¹⁷, P. GIOMMI¹⁷, S. COLAFRANCESCO¹⁷, L. A. ANTONELLI¹⁸, AND L. SALOTTI¹⁹

¹ INAF/IASF-Roma, I-00133 Roma, Italy

² Dipartimento di Fisica, Università di Roma Tor Vergata, I-00133 Roma, Italy

³ INAF/IASF-Milano, I-20133 Milano, Italy

⁴ CIFS-Torino, I-10133 Torino, Italy

⁵ Dipartimento di Fisica and INFN Trieste, I-34127 Trieste, Italy

⁶ INAF/IASF-Bologna, I-40129 Bologna, Italy

⁷ INFN-Pavia, I-27100 Pavia, Italy

⁸ Dipartimento di Fisica, Università di Torino, Turin, Italy

⁹ ENEA-Bologna, I-40129 Bologna, Italy

¹⁰ INFN-Roma La Sapienza, I-00185 Roma, Italy

¹¹ CNR-IMIP, Roma, Italy

¹² INFN Roma Tor Vergata, I-00133 Roma, Italy

¹³ INAF-Osserv. Astron. di Cagliari, I-09012 Capoterra, Italy

¹⁴ Dipartimento di Fisica, Università dell’Insubria, I-22100 Como, Italy

¹⁵ ENEA Frascati, I-00044 Frascati, Roma, Italy

¹⁶ INAF/IASF Palermo, Italy

¹⁷ ASI Science Data Center, I-00044 Frascati, Roma, Italy

¹⁸ INAF-Osserv. Astron. di Roma, Monte Porzio Catone, Italy

¹⁹ Agenzia Spaziale Italiana, I-00198 Roma, Italy

Received 2009 August 17; accepted 2010 January 21; published 2010 February 3

ABSTRACT

The supernova remnant (SNR) IC 443 is an intermediate-age remnant well known for its radio, optical, X-ray, and gamma-ray energy emissions. In this Letter, we study the gamma-ray emission above 100 MeV from IC 443 as obtained by the *AGILE* satellite. A distinct pattern of diffuse emission in the energy range 100 MeV–3 GeV is detected across the SNR with its prominent maximum (source “A”) localized in the northeastern shell with a flux $F = (47 \pm 10) \times 10^{-8}$ photons $\text{cm}^{-2} \text{s}^{-1}$ above 100 MeV. This location is the site of the strongest shock interaction between the SNR blast wave and the dense circumstellar medium. Source “A” is *not* coincident with the TeV source located 0.4° away and associated with a dense molecular cloud complex in the SNR central region. From our observations, and from the lack of detectable diffuse TeV emission from its northeastern rim, we demonstrate that electrons cannot be the main emitters of gamma rays in the range 0.1–10 GeV at the site of the strongest SNR shock. The intensity, spectral characteristics, and location of the most prominent gamma-ray emission together with the absence of cospatial detectable TeV emission are consistent only with a hadronic model of cosmic-ray acceleration in the SNR. A high-density molecular cloud (cloud “E”) provides a remarkable “target” for nucleonic interactions of accelerated hadrons; our results show enhanced gamma-ray production near the molecular cloud/shocked shell interaction site. IC 443 provides the first unambiguous evidence of cosmic-ray acceleration by SNRs.

Key words: cosmic rays – gamma rays: general – ISM: supernova remnants – supernovae: general – supernovae: individual (IC 443)

1. INTRODUCTION

Galactic cosmic rays (CRs) are believed to be accelerated above 10^{14} – 10^{15} eV energies by powerful supernovae (SNe) in our Galaxy (e.g., Shklovskii 1953; Ginzburg & Syrovatskij 1964; Cesarsky 1980; Blandford & Eichler 1987), and gamma rays above 70 MeV are expected to provide the crucial signature of hadronic acceleration. Shock-accelerated CRs interacting with the gaseous surroundings of supernova remnants (SNRs) produce gamma rays by nucleon–nucleon interactions and neutral–pion decay. Indeed, EGRET observations of SNRs have provided several important gamma-ray/SNR associations (Sturmer & Dermer 1995; Esposito et al. 1996). However, the

complex morphology of SNRs and the EGRET angular resolution prevented a definite resolution of this issue (e.g., Torres et al. 2003). In recent years, TeV detections of SNRs provided additional and very promising elements (e.g., Aharonian 2004; Aharonian et al. 2007a, 2007b, 2008; Yamazaki et al. 2006; Enomoto et al. 2006; Berezhko & Völk 2006; Albert et al. 2007, 2008; Acciari et al. 2009). However, the hadronic interpretation of these detections usually requires the knowledge of SNR physical parameters or processes (e.g., electrons’ bremsstrahlung/inverse Compton emission versus hadronic pion production, magnetic field strengths, the electron/proton number ratio for GeV–TeV kinetic energies, etc.). Difficulties in the interpretation of SNR gamma-ray and TeV data remain because of our

poor knowledge of SNR distances and ages, ambient gas density, and problematic determinations of the non-thermal synchrotron and high-energy emissions.

To unambiguously prove the CR acceleration by SNe, we need SNRs for which we can demonstrate that the ubiquitous and co-accelerated electrons do not dominate the observed gamma-ray and TeV emission. Given the variety of SNRs and the complexity of interactions with their environments, this task turned out to be very difficult to accomplish.²⁰

Current gamma-ray instrumentation can substantially improve this picture. Detailed gamma-ray mapping of SNRs can provide a first piece of evidence, i.e., confirming whether pion-generated emission in the energy range 100 MeV–10 GeV is mostly concentrated in sites where molecular clouds are strongly shocked by SNR expanding shells. As mentioned above, a second piece of evidence is required, showing that hadrons and not electrons are the main contributors to the detected gamma-ray emission. It turns out that IC 443 provides both pieces of evidence.

2. THE SUPERNOVA REMNANT IC 443

The intermediate age SNR IC 443 ($\tau \sim 10$ – 20 thousand years) is located near the Galactic anticenter ($l = 189.1$, $b = +3.0$), and is at a relatively close distance from the Earth (~ 1.5 kpc; Welsh & Sallmen 2003). It is one of the best studied SNRs because of its complex structure and interaction with its gaseous surroundings in the absence of strong diffuse Galactic emission. Radio (Mufson et al. 1986; Leahy 2004), optical (Fesen & Kirshner 1980), and X-ray (e.g., Petre et al. 1988; Asaoka & Aschenbach 1994; Kawasaki et al. 2002; Troja et al. 2006) mapping of the SNR shows an asymmetric shape. The northeast rim expands in a relatively dense environment with a shock velocity of $v_s \sim 65$ – 100 km s⁻¹ (for an average number density of the unperturbed medium $n_1 \sim 10$ – 100 cm⁻³; Fesen & Kirshner 1980), and the southwest shell expands in a much more dilute medium ($n_2 \sim 1$ – 10 cm⁻³). In the middle of the SNR, a dense and very massive ($\sim 1000 M_\odot$) molecular cloud complex in the form of a torus or “ring” surrounds the expanding supernova (SN) shell from the exterior (Dickman et al. 1992; Lee et al. 2008). Carbon monoxide (CO) mapping of IC 443 shows several other smaller molecular clouds that interact with the expanding shell. In particular, the molecular cloud complex named “E” with a projected size of ~ 1 pc and mass estimate which equals $23 M_\odot$ is the only prominent mass clump located just in front of the expanding SN shell in the northeastern rim (Dickman et al. 1992). Furthermore, detailed mapping of the $J = 1 - 0$ line of the formyl ion (HCO⁺, which traces compressed and heated gas within the SNR) clearly shows that both the massive “ring” and the cloud “E” physically interact with the SN ejecta. Given the morphology of the SNR and its molecular clouds environment, IC 443 is therefore an ideal system to test the hypothesis of hadronic CR acceleration in SNRs. It provides a system which has all the required ingredients: a powerful SN of total explosion energy $W \sim 10^{51}$ erg, both dilute and dense ambient gaseous environments surrounding the SN blast wave, and a complex of molecular clouds physically interacting with the SN shock.

3. AGILE GAMMA-RAY OBSERVATIONS OF IC 443

The *AGILE* satellite has been operating since 2007 April 23 (Tavani et al. 2009). The *AGILE* scientific instrumentation

is very compact and is based on two co-aligned imaging detectors operating in the energy ranges 30 MeV–30 GeV (GRID; Barbiellini et al. 2002; Prest et al. 2003) and 18–60 keV (Super-*AGILE*; Feroci et al. 2007). An anticoincidence system (Perotti et al. 2006), a calorimeter (Labanti et al. 2006), and a data-handling system (Argan et al. 2004) complete the instrument. *AGILE*'s performance is characterized by very large fields of view (2.5 and 1 sr for the gamma-ray and hard X-ray bands, respectively), optimal angular resolution, and good sensitivity (see Tavani et al. 2009 for details about the mission and main instrument performance).

During the first two years of operations, *AGILE* observed the Galactic anticenter region several times. A total observing time of approximately 1 Ms was accumulated by *AGILE*, on IC 443, and a high-resolution mapping and spectral analysis in the energy range 100 MeV–20 GeV were obtained using standard *AGILE* gamma-ray selection procedures. Positional astrometry has carefully been checked by comparing the IC 443 gamma-ray emission with the nearby Crab and Geminga pulsars.

The region is not substantially affected by the weak diffuse gamma-ray Galactic emission that is properly taken into account in our analysis (Giuliani et al. 2004).

Figure 1 shows the result of the *AGILE* detailed gamma-ray mapping (above 400 MeV) superimposed to an optical map of the northeastern rim of IC 443. Diffuse gamma-ray emission with significant enhancements is detected across IC 443 in a pattern that closely resembles the SNR outer shell configuration. A most prominent gamma-ray enhancement (that we label “source A” in Figure 1) is clearly detected in the northeastern region of IC 443 at a location coincident with the most active expanding SN blast wave. We also detect several other gamma-ray enhancements that follow a pattern surrounding the outer regions of the SNR shell. We label the remaining enhancements “B,” “C,” and “D” (see Figure 1). The gamma-ray pattern of emission from IC 443 does not show any sign of significant variability. In this Letter, we concentrate our analysis on the northeastern rim of IC 443 and on source “A,” postponing a more detailed study of the SNR to a forthcoming publication.

Source “A” is detected at the 11σ level at the Galactic coordinate location (l,b): $(189.08, 3.28) \pm 0.17$ (stat.) ± 0.1 (syst.) with a flux $F = (47 \pm 10) \times 10^{-8}$ photons cm⁻² s⁻¹ above 100 MeV. We note that the position of source “A” is consistent with that of the only prominent molecular cloud in the northeastern region, i.e., cloud “E” of Dickman et al. (1992) which is in physical interaction with the expanding shell. Clearly marked in Figure 1 is the relatively small error box of the most prominent TeV source detected by MAGIC (Albert et al. 2007) and VERITAS (Acciari et al. 2009). The pulsar wind nebula CXOU J061705.3–222127 (Gaensler et al. 2006) is not associated with any prominent gamma-ray emission.

Within the statistical and systematic uncertainties, the source “A” location is consistent with the EGRET (3EG J10617+2238; Hartman et al. 1999), *AGILE* (AGL J0617+2236; Pittori et al. 2009), and *Fermi-Large Area Telescope* (0FGL J0617.4+2234; Abdo et al. 2009) sources. While the EGRET source appeared to be marginally compatible with the position of the TeV source, the refined *AGILE* location is inconsistent at more than the 99% confidence level with that of the TeV source. The location of the most intense TeV emission is indeed concentrated in the central part of IC 443 in apparent superposition with the massive molecular cloud “ring.” The angular distance between source “A” and the TeV source centroid is more than 0.4° , i.e., significantly larger than the location accuracies of *AGILE* (0.1°).

²⁰ See also Butt (2009), for a recent review.

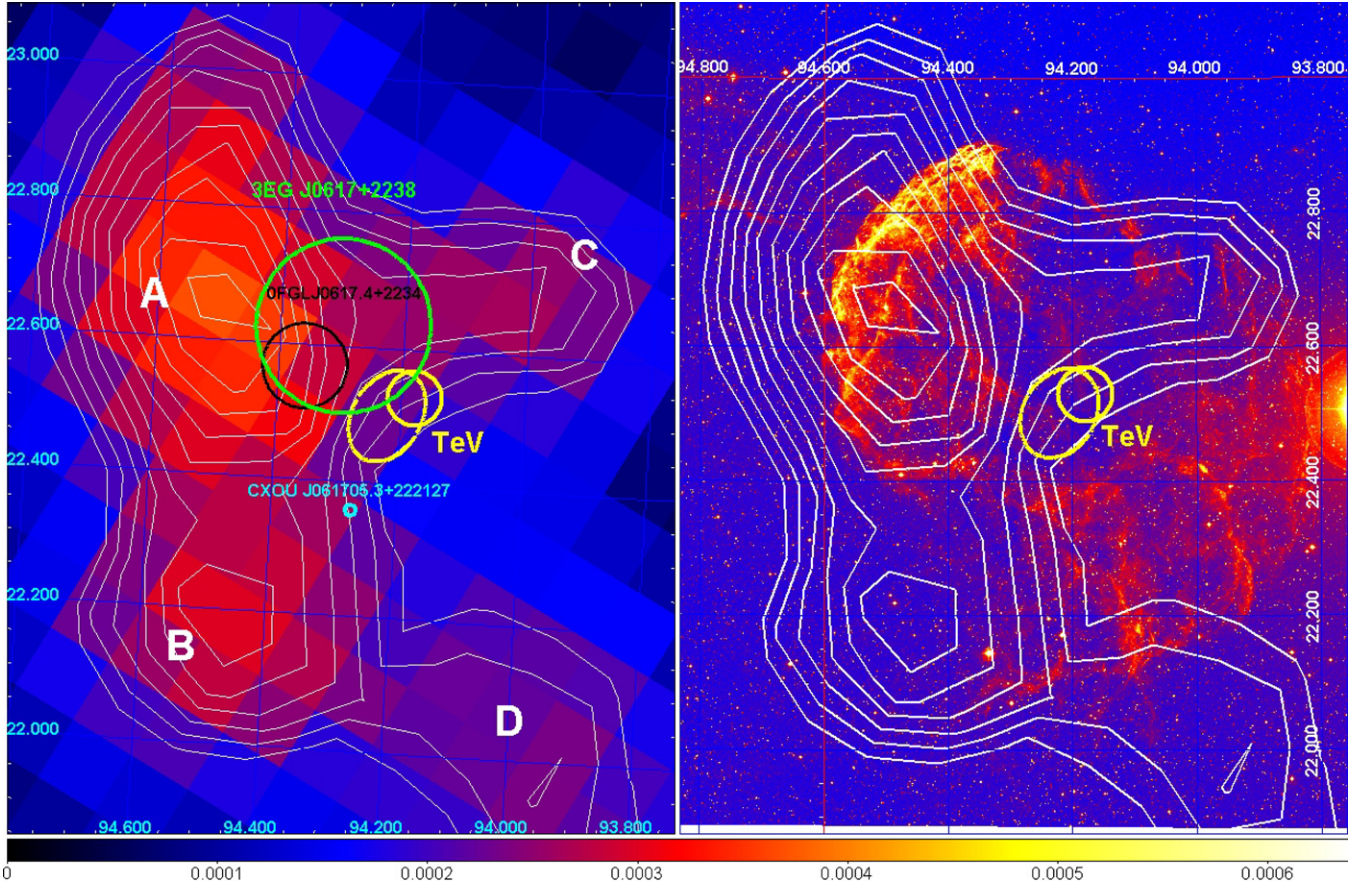


Figure 1. Gamma-ray intensity maps (J2000 R.A. and decl. coordinates) above 400 MeV of IC443 obtained by integrating all *AGILE* data. Left panel: gamma-ray intensity map above 400 MeV centered on IC 443. The color bar scale is in units of photons $\text{cm}^{-2} \text{s}^{-1} \text{pixel}^{-1}$. Pixel size is 0.1, and we used a three-bin Gaussian smoothing. White contour levels of the gamma-ray intensity start from 0.0002 and increase in steps of 0.000173. We also mark the positions and circular approximations of the 95% error boxes of the EGRET source 3EG J0617+2238 (green circle) and *Fermi*-LAT 0FGL J0617.4+2234 (black circle). The position of the TeV source associated with IC 443 is marked by a yellow circle and ellipse that give the 95% confidence level error boxes determined by MAGIC (Albert et al. 2007) and VERITAS (Acciari et al. 2009), respectively (see also Butt 2009). The X-ray source CXOU J061705.3+222127 is marked by a cyan circle. Right panel: optical image of IC 443 (Palomar Digitized Sky Survey) superimposed with the *AGILE* gamma-ray intensity contours above 400 MeV (same as the left panel). The position of the TeV source is marked by the yellow circle (MAGIC) and ellipse (VERITAS). The angular distance between the centroids of the gamma-ray dominant source in the northeastern rim and the TeV source is ~ 0.4 . The TeV source is located in the central part of the IC 443 at the location coincident with a massive molecular cloud complex (Dickman et al. 1992). At the estimated distance of 1.5 kpc, 1 arcmin subtends a distance of 0.44 pc.

for this integration) and of MAGIC and VERITAS. We conclude that the positional difference between the gamma-ray source “A” and the TeV source is significant and reflects the difference in the physical locations of the dominant 0.1–10 GeV and TeV emissions, respectively. We infer a very important fact for the physical interpretation of our observations; the most prominent 100 MeV–10 GeV emission is not cospatial with the TeV source. Furthermore, *AGILE* detects weak and diffuse gamma-ray emission from the central location of IC 443 in coincidence with the TeV source and the centroid of the massive molecular “ring.”

4. DISCUSSION

Let us denote by $\chi_{e,p}$ the ratio between the electron and hadron number density normalizations (at momentum $p = 1 \text{ GeV}/c$). Electrons can emit high-energy photons by bremsstrahlung and inverse Compton (IC) scattering. Emission by these two processes is unavoidably linked, in the sense that if an electron bremsstrahlung contribution emerges as a prominent spectral component, a strong IC contribution is predicted in the TeV range. The same electrons emitting bremsstrahlung gamma rays (possibly enhanced by a dense cloud) also unavoidably

scatter the ambient optical/IR photon bath of the SNR/interstellar medium and the cosmic microwave background (CMB) photons. A general conclusion can be deduced for a typical SNR: a ratio $\chi_{e,p} \sim 1$ implies *cospatial* 100 MeV and TeV emissions in SNRs. A detailed modeling of electron (and proton) emissivities of IC 443 indeed predicts that for an ideal matter density of $n_o \sim 1 \text{ cm}^{-3}$ the IC contribution to the spectral power (νF_ν) dominates by a factor of ~ 10 over the bremsstrahlung contribution for photon energies between 100 MeV and 1 GeV (Gaisser et al. 1998, GPS98). For higher energies, the IC dominance is even larger, leading to a predicted IC power at 300 GeV larger than a factor of ~ 100 , than the bremsstrahlung spectral power. If we apply these predictions to the specific case of the IC 443 northeastern rim characterized by an external medium density $n_1 \sim 10\text{--}100 \text{ cm}^{-3}$, we expect the bremsstrahlung power (νF_ν)_B near 0.1–1 GeV and the IC power (νF_ν)_{IC} near 0.3–1 TeV to be approximately equal. This implies that a model with $\chi_{e,p} \sim 1$ predicts the electron-driven TeV emission to be cospatial with the northeastern rim, and in particular to be coincident with the 0.1–1 GeV emission. Since this is not observed, we conclude that the SNR shock must be characterized by a ratio $\chi_{e,p}$ substantially less than unity. We note that a value $\chi_{e,p} \sim 0.01$ has indirectly been deduced for IC 443

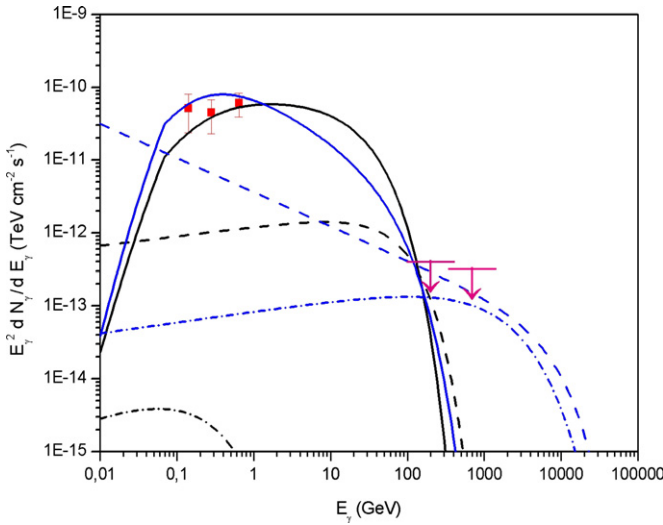


Figure 2. *AGILE* gamma-ray spectrum (between 100 MeV and 1 GeV) and the TeV upper limits of the region centered at the source “A” of IC 443 compared with two different models for the gamma-ray emissivities. Solid curves: hadronic production of gamma rays by neutral pion decay (blue curve: model 1; black curve: model 2). Dashed curves: bremsstrahlung emission by electrons (blue curve: model 1; black curve: model 2). Short-dash-dot curves: electron IC emission on the CMB (blue curve: model 1; black curve: model 2). The MAGIC upper limits are assumed to have values three times smaller than the reported flux levels of the TeV source at the center of IC 443 (Albert et al. 2007; Acciari et al. 2009). The *AGILE* spectral data agree with those reported by EGRET (Esposito et al. 1996).

(GPS98) and other SNRs (e.g., Aharonian 2004), and in general agrees with what is observed in direct CR measurements.

The overall pattern of gamma-ray emission from IC 443, combined with the absence of detectable cospatial TeV emission both near source “A” and over the whole semispherical shocked northeastern rim, has far-reaching consequences. Figure 2 shows the results of two leading models of gamma-ray emissivity produced by protons and electrons near source “A.” We follow the treatment of Drury et al. (1994) and Berezhko & Völk (1997) for the normalization of the expected gamma-ray emission from accelerated hadronic CRs in terms of parameters of the late SNR evolutionary phase giving $E_\gamma^2 dN_\gamma/dE_\gamma \simeq 5 \times 10^{-11} (\text{TeV cm}^{-2} \text{s}^{-1}) (E_{\text{SN}}/10^{51} \text{ erg}) (d/1 \text{ kpc})^{-2} n_1 f$, where E_{SN} is the total SN explosion energy, d is the source distance, and f is a geometrical factor. For simplicity, we assume that hadrons and electrons are accelerated at the northeastern shock with the same power-law energy index, i.e., $N(E) = k E^{-\alpha}$. Models without energy cutoffs below 10 TeV for both electrons ($E_{c,e}$) and protons ($E_{c,p}$) contradict the observations. We consider then two models²¹ for source “A” as constrained by the data with $E_{\text{SN}} = 10^{51}$ erg, $d = 1.5$ kpc, and $f \simeq 0.01$. Model 1 is characterized by $\chi_{e,p} = 0.03$, $\alpha = 2.7$, $n_1 = 10^3 \text{ cm}^{-3}$, $E_{c,e} = 10$ TeV, and $E_{c,p} = 200$ GeV. Model 2 has $\chi_{e,p} = 0.01$, $\alpha = 2.1$, $n_1 = 10^3 \text{ cm}^{-3}$, $E_{c,e} = 100$ GeV, and $E_{c,p} = 100$ GeV. Figure 2 clearly shows that the hadron-produced gamma-ray emissivity has to be suppressed between 10 and 100 GeV. The electron bremsstrahlung and IC contributions are also shown; both have to be consistent with the absence of cospatial gamma-ray and TeV emission in the northeastern rim satisfying the observational constraint

$\nu F_\nu(100 \text{ MeV} - 10 \text{ GeV}) \gtrsim 100 \nu F_\nu(0.2 - 1 \text{ TeV})$. We note that a value of $\chi_{e,p} \sim 0.01$ is consistent with the radio synchrotron emission observed in the northeastern part of the IC 443 shell (Erickson & Mahoney 1985) for an average local magnetic field $B \sim 10^{-5}$ G.

5. CONCLUSIONS

We obtain a satisfactory physical picture of IC 443 with very important implications for the problem of the cosmic-ray production by SNRs. Diffuse gamma-ray emission of hadronic origin is remarkably distributed in coincidence with the IC 443 outer shock. A clear gamma-ray enhancement is detected (source “A”) in the northeastern rim and close to the molecular cloud “E.” This cloud provides an ideal target for nucleonic interactions of accelerated hadrons (protons and ions) with subsequent gamma-ray emission by neutral pion decay. Cloud “E” has a substantial target matter density for efficient hadronic interaction with a timescale $\tau_{pp \rightarrow \pi^0} \sim (5 \times 10^4 \text{ yr}) (n/10^3 \text{ cm}^{-3})^{-1}$. This timescale turns out to be comparable with the age of the remnant and implies a high efficiency of gamma-ray production by the SN blast wave–cloud interaction. By assuming an average particle kinetic energy of the order of 0.1–1 TeV, our gamma-ray observations of IC 443 and the proposed physical interpretation are in agreement with the total energy in cosmic-ray particles being 1%–10% of the total estimated SN explosion energy of about 10^{51} erg.

At the source “A” site, both the proton and electron distributions have an effective energy cutoff on the order of 100 GeV. We note that several models of particle acceleration in high-density regions close to the acceleration site consider the possibility of effective energy cutoffs of the order 0.1–1 TeV (e.g., Drury et al. 1996; Baring et al. 1999; Malkov et al. 2002). These effective cutoffs can be caused by a combination of inefficient acceleration at larger energies and particle diffusion. The CR maximum kinetic energy E_m produced by shock acceleration can be estimated as $D(E_m) = R_s V_s / k'$, where $D(E)$ is the particle spatial diffusion coefficient, $k' \simeq 30$ for the late evolutionary phase, and R_s and V_s are the shock radius and speed, respectively (e.g., Berezhko 1996). An upper limit for E_m applicable to source “A” of IC 443 can be obtained with a Bohm approximation for D , and $R_s = 1$ pc, $V_s \sim 10^8 \text{ cm}^{-2} \text{ s}^{-1}$, and $B \sim 5 \times 10^{-6}$ G. We obtain $E_m \sim 1$ TeV, indicating that the active SNR shocked region currently contains only relatively low kinetic energy particles with the highest energy CRs diffused away long ago. Our observations of the intermediate-age IC 443 support this important aspect of the particle acceleration mechanism.

It is also interesting to address the lack of prominent gamma-ray emission in coincidence with the TeV source in the high-density medium at the center of the SNR. A possible explanation is based on a combination of energy-dependent particle diffusion and nucleonic interactions in the very dense central medium reached by the SN shock (Torres et al. 2008). In any case, the absence of detectable TeV emission from most of the SNR argues for a sub-dominant electron contribution to the emission.

We presented here two specific emission models in agreement with the high-energy observations and yet predicting different fluxes in the TeV range. Future deep TeV observations of IC 443 may reveal a weak TeV emission associated with the northeastern rim and the source “A” region. Figure 2 provides an example of how these observations may help in further constraining the theoretical models.

²¹ In order to display the dynamic range of the most important parameter influencing the shape of the spectrum, we consider the values $\alpha = 2.1$ (a realistic case) and $\alpha = 2.7$ (a case with no spatial diffusion).

IC 443 turns out to be the first SNR clearly providing evidence for hadronic cosmic-ray acceleration and interaction with its gaseous surroundings. A leptonic model of emission is in contradiction with the combined gamma-ray/TeV observations of the northeastern rim of IC 443 and in particular of the source “A” region. A hadronic model of emission agrees in a natural way with our observations and confirms the hypothesis that SN blast waves can efficiently accelerate protons and possibly other ions in our Galaxy.

We thank an anonymous referee for his/her comments that led to an improvement in the discussion of our results. The *AGILE* Mission is funded by the Italian Space Agency (ASI) with scientific and programmatic participation by the Italian Institute of Astrophysics (INAF) and the Italian Institute of Nuclear Physics (INFN). This investigation was carried out with partial support from the ASI contract no. I/089/06/2.

REFERENCES

- Abdo, A. A., et al. 2009, <http://fermi.gsfc.nasa.gov>
- Acciari, V. A., et al. 2009, *ApJ*, **698**, L133
- Aharonian, F. A. 2004, Very High Energy Cosmic Gamma Radiation (Singapore: World Scientific)
- Aharonian, F. A., et al. 2007a, *A&A*, **464**, 235
- Aharonian, F. A., et al. 2007b, *ApJ*, **661**, 236
- Aharonian, F. A., et al. 2008, *A&A*, **481**, 401
- Albert, J., et al. 2007, *ApJ*, **664**, L87
- Albert, J., et al. 2008, *ApJ*, **674**, 1037
- Argan, A., et al. 2004, Proc. IEEE-NSS, **1**, 371
- Asaoka, I., & Aschenbach, B. 1994, *A&A*, **284**, 573
- Barbiellini, G., et al. 2002, *Nucl. Instrum. Methods Phys. Res. A*, **490**, 146
- Baring, M. G., Ellison, D. C., Reynolds, S. P., Grenier, I. A., & Goret, P. 1999, *ApJ*, **513**, 311
- Berezhko, E. G. 1996, *Astropart. Phys.*, **5**, 367
- Berezhko, E. G., & Völk, H. J. 1997, *Astropart. Phys.*, **14**, 183
- Berezhko, E. G., & Völk, H. J. 2006, *A&A*, **451**, 981
- Blandford, R., & Eichler, D. 1987, *Phys. Rep.*, **154**, 1
- Butt, Y. 2009, *Nature*, **460**, 701
- Cesarsky, C. J. 1980, *ARA&A*, **18**, 289
- Dickman, R. L., Snell, R. L., Ziurys, L. M., & Huang, H. L. 1992, *ApJ*, **400**, 203
- Drury, L. O’C., Aharonian, F. A., & Voelk, H. J. 1994, *A&A*, **287**, 959
- Drury, L. O’C., Duffy, P., & Kirk, J. G. 1996, *A&A*, **309**, 1002
- Enomoto, R., et al. 2006, *ApJ*, **652**, 1268
- Erickson, W. C., & Mahoney, M. J. 1985, *ApJ*, **290**, 596
- Esposito, J. A., Hunter, S. D., Kanbach, G., & Sreekumar, P. 1996, *ApJ*, **461**, 820
- Feroci, M., et al. 2007, *Nucl. Instrum. Methods Phys. Res. A*, **581**, 728
- Fesen, R. A., & Kirshner, R. P. 1980, *ApJ*, **242**, 1023
- Gaensler, B. M., Chatterjee, S., Slane, P. O., van der Swaluw, E., Camilo, F., & Hughes, J. P. 2006, *ApJ*, **648**, 1037
- Gaisser, T. K., Protheroe, R. J., & Stanev, T. 1998, *ApJ*, **492**, 219
- Ginzburg, V. L., & Syrovatskij, S. I. 1964, The Origin of Cosmic Rays (New York: Pergamon Press)
- Giuliani, A., et al. 2004, Mem. Soc. Astron. Ital., **5**, 135
- Hartman, R. C., et al. 1999, *ApJS*, **123**, 79
- Kawasaki, M. T., et al. 2002, *ApJ*, **572**, 897
- Labanti, C., et al. 2006, Proc. SPIE, **6266**, 62663
- Leahy, D. A. 2004, *AJ*, **127**, 2277
- Lee, J.-J., et al. 2008, *AJ*, **135**, 796
- Malkov, M. A., Diamond, P. H., & Jones, T. W. 2002, *ApJ*, **571**, 856
- Mufson, S. L., et al. 1986, *AJ*, **92**, 1349
- Perotti, F., et al. 2006, *Nucl. Instrum. Methods Phys. Res. A*, **556**, 228
- Petre, R., Szymkowiak, A. E., Seward, F. D., & Willingale, R. 1988, *ApJ*, **335**, 215
- Pittori, C., et al. 2009, *A&A*, **506**, 1563
- Prest, M., et al. 2003, *Nucl. Instrum. Methods Phys. Res. A*, **501**, 280
- Shklovskii, I. S. 1953, Dokl. Akad. Nauk SSSR, **91**, 475
- Sturmer, S. J., & Dermer, C. D. 1995, *A&A*, **293**, 17
- Tavani, M., et al. 2009, *A&A*, **502**, 995
- Torres, D. F., Marrero, A. Y., & Cea del Pozo, E. 2008, MNRAS, **387**, L59
- Torres, D. F., Romero, G. E., Dame, T. M., Combi, J. A., & Butt, Y. M. 2003, *Phys. Rep.*, **382**, 303
- Troja, E., Bocchino, F., & Reale, F. 2006, *ApJ*, **649**, 258
- Welsh, B. Y., & Sallmen, S. 2003, *A&A*, **408**, 545
- Yamazaki, R., et al. 2006, MNRAS, **371**, 1975